Interchannel Interference in Multiwavelength Operation of Integrated Acousto-Optical Filters and Switches

F. Tian and H. Herrmann

Abstract—Multiple wavelength filtering/switching can be obtained using integrated acousto-optical wavelength filters and switches in LiNbO$_3$ by driving them with several RF signals simultaneously. As a consequence, interchannel interference occurs due to the interaction of several acoustic waves within the same mode converter resulting in an intensity modulation of the transmitted optical waves. System performance can be degraded as this interchannel interference leads to a power penalty equivalent to an additional cross talk. We present the coupled-mode analysis of the interchannel interference in the multiwavelength operation of acousto-optical filters and switches. Theoretical models are developed and confirmed by experimental results. Furthermore, the impact on WDM system performance is studied by measuring bit error rate characteristics and comparing the results with the theory.

I. INTRODUCTION

Integrated acousto-optically tunable filters (IAOTF) and switches (IAOTS) in LiNbO$_3$ have potential applications in wavelength division multiplexed (WDM) optical networks [1]–[3]. They offer unique properties for the construction of new WDM network architectures: broad and electronic tunability [4], narrow channel spacing [7], simultaneous multiwavelength filtering/switching [8], [9], and gain equalizing [10].

The basic element of such integrated acousto-optical devices is the acousto-optical mode converter (Fig. 1). Via an interaction between a surface acoustic wave (SAW) and the optical waves, a polarization conversion can be achieved. As this process requires phase-matching, it is strongly wavelength-selective.

An important aspect for WDM applications of IAOTF's and IAOTS's is the cross talk induced by these devices. There are two kinds of cross talk in multiwavelength operation of such devices: The first one is an intensity cross talk which is apparent in single channel operation, too. Its source is some residual conversion at the wavelengths of the neighboring channels due to sidelobes of the acousto-optical conversion characteristics. Similar to the single channel operation, this kind of cross talk can be greatly reduced by using double-stage IAOTF's [5]–[7] or by using weighted coupling schemes [11], [12]. The second

cross talk is generated by the interchannel interference of two or more acoustic waves simultaneously travelling along the acousto-optical interaction region, which results in an intrinsic modulation of the transmitted signal. It has been observed experimentally that this interchannel interference degrades the bit-error-rate (BER) of WDM systems using IAOTF's [13], especially at narrow channel spacing.

A qualitative interpretation of the phenomenon of interchannel interference is given in [13]. It is assumed that two SAW's at frequencies f_1 and f_2 are excited in a mode converter yielding a conversion at the wavelengths λ_1 and λ_2, respectively, as indicated in the right diagram in Fig. 1. Due to sidelobes of the conversion characteristics a residual conversion resulting from the SAW at f_1 is induced at λ_2 and vice versa. As the acousto-optical conversion process is accompanied by a frequency shift of the converted wave by the frequency of the SAW, the optical wave at λ_1 is mainly shifted by f_1 but a small fraction is shifted by f_2. This results in a beating of the transmitted amplitude, which can be interpreted as an amplitude modulation of the transmitted optical wave. But this interpretation can not explain the experimental results that a relatively large power penalty occurs even if the second channel is placed at the first channel transmission null and that there exist higher order harmonics in the modulated signal.

Another picture for a qualitative explanation of interchannel interference is based on the interference of two travelling gratings. Each SAW generates a travelling grating with a period given by the acoustical wavelength. If two SAW's are excited the corresponding gratings (with different periods) interfere with each other resulting in a time-dependent acousto-optical coupling strength and, therefore, in a time-dependent efficiency of the conversion process. As a consequence, the power of the converted wave must be modulated.

In this paper we present a detailed analysis of interchannel interference in multiwavelength operation of IAOTF's/IAOTS's. In Section II, two theoretical models based on coupled mode analysis will be developed—one is in the time domain and the other in the frequency domain—which describe the process of interchannel interference and allow the modeling for various configurations of filters and switches. In Section III experimental results of intensity modulated transmission will be given and compared with theoretical results. The influence on BER in transmission systems due to interchannel interference will be discussed in Section IV. Both, theoretical and experimental results will be given.
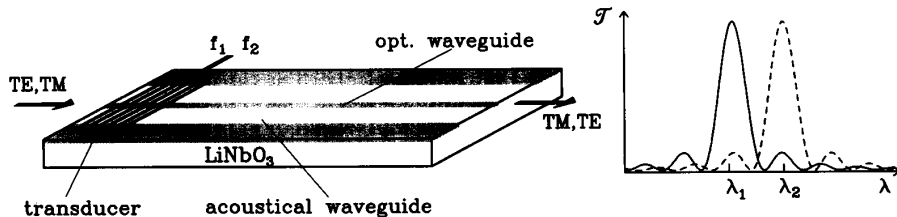
Fig. 1. Integrated acoustooptical TE/TM converter in LiNbO₃. By applying two RF-signals at frequencies f_1 and f_2 a conversion occurs at wavelengths λ_1 and λ_2 as sketched in the right diagram.

II. THEORETICAL MODELS

It is well known that in an IAOTF/IAOTS the selection of optical channels is accomplished by means of a narrow-band resonant acousto-optical polarization conversion of light. Both kinds of cross talk in multiwavelength operation are induced in the process of acousto-optic interaction. In the following, we will employ the coupled-mode theory to treat the interchannel interference in acousto-optical polarization conversion.

In general, the differential equations that describe codirectional coupling of two optical modes due to their interaction with a single acoustic wave are [14]

$$\frac{\partial A}{\partial z} = -j\kappa^* B \, \exp\left(-j\delta z\right) \qquad (1)$$

$$\frac{\partial B}{\partial z} = -j\kappa A \, \exp\left(j\delta z\right) \qquad (2)$$

where A and B are slowly varying amplitudes of TE- and TM-polarized waves which have propagation constants β_{TE} and β_{TM}, respectively. κ is the coupling coefficient; it can be assumed to be constant for an acousto-optical mode converter with homogeneous coupling but will be a sinusoidal function, if a converter with acoustical directional coupler for weighted coupling is considered [11], [12]. $\delta = \beta_{TM} - \beta_{TE} - K$ (where K is the propagation constant of the surface acoustic wave with a space and time evolution proportional to $\exp\left[j(\Omega_a t - Kz)\right]$, and $\Omega_a = 2\pi f_a$ is the angular frequency of the surface acoustic wave).

When several acoustic waves are travelling simultaneously along the acousto-optical interaction region, they interfere with each other. The Eqns. (1) and (2) have to be modified. The acousto-optical interaction for such situations can be treated theoretically in the frequency and in the time domain. For both, theoretical models will be described. For simplicity, we assume in the following that two codirectional acoustic waves are running with same amplitude but different propagation constants K_1 and K_2 and frequencies Ω_1 and Ω_2, respectively.

The first model is based on an analysis in the time domain. The linear superposition of two acoustic waves creates a time-dependent interference pattern which can be interpreted as a modulated travelling diffraction grating with an average propagation constant $K_0 = (K_1 + K_2)/2$ in the interference area:

$$\exp\left[j(\Omega_1 t - K_1 z)\right] + \exp\left[j(\Omega_2 t - K_2 z)\right] =$$
$$2\cos\left[\frac{\Delta K}{2}z - \frac{\Delta\Omega}{2}t\right]\exp\left[j(\Omega_0 t - K_0 z)\right] \qquad (3)$$

Here, the abbreviations $\Delta\Omega = \Omega_1 - \Omega_2$, $\Omega_0 = (\Omega_1 + \Omega_2)/2$ and $\Delta K = K_1 - K_2$ have been used. Direct comparison with the case of a single acoustic wave leads to the following modified coupling equations

$$\frac{\partial A}{\partial z} = -j2\kappa^* \cos\left[\frac{\Delta K}{2}z - \frac{\Delta\Omega}{2}t\right]B \, \exp\left(-j\delta z\right) \qquad (4)$$

$$\frac{\partial B}{\partial z} = -j2\kappa \cos\left[\frac{\Delta K}{2}z - \frac{\Delta\Omega}{2}t\right]A \, \exp\left(j\delta z\right) \qquad (5)$$

with $\delta = \beta_{TM} - \beta_{TE} - K_0$.

Comparing (1) and (2) with (4) and (5), we see that the time-independent coupling is replaced by a time-dependent and space weighted coupling in (4) and (5) which results in an amplitude- and frequency-modulation of coupled optical waves.

The wavelength selective characteristics of IAOTF's/IAOTS's can be calculated numerically based on (4) and (5). The power transmission of converted and nonconverted light are periodic functions of time with a periodicity of $T_0 = 2\pi/\Delta\Omega$. As we want to study the spectral properties in the subsequent section, we expand the transmission function of the converted light in a Fourier series, i.e.

$$T_1(t) = \sum_{n=-\infty}^{\infty} C_n \, \exp\left(jn\Delta\Omega t\right). \qquad (6)$$

Another possibility is to describe the conversion process in the frequency domain. The acousto-optical conversion is—as required by energy conservation—accompanied by a frequency shift of the converted optical wave by exactly the acoustic frequency; the direction of the shift depends on the polarization of converted light and the propagation direction of the SAW relative to that of the optical waves. If, for example, two SAW's with angular frequencies Ω_1 and Ω_2 are involved in the acousto-optical interaction process, a series of optical waves at different discrete frequencies are generated. This is illustrated in Fig. 2. Starting, for example, with input $A(0)$, i.e., polarization state A (TE) and frequency shift 0, the signal fans out to several components. Via the interaction with the SAW's at Ω_1 and Ω_2, optical waves $B(\Omega_1)$ and $B(\Omega_2)$ are generated. These waves couple again to the polarization state A with frequency shifts $\Omega_2 - \Omega_1$, 0 and $\Omega_1 - \Omega_2$. And the acousto-optical interaction with these waves generates optical waves in the polarization state B with new frequency components and so on. This means, a set of optical waves in the polarization state A with frequency shifts 0, $\pm 2(\Delta\Omega/2)$,
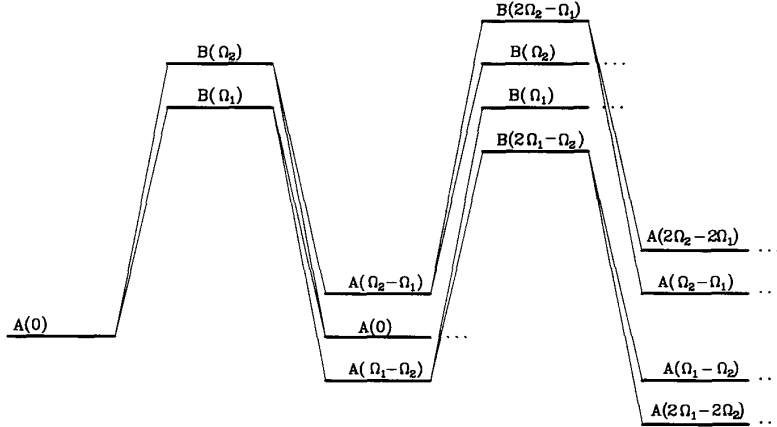
Fig. 2. Coupling scheme for the two frequency operation of an acousto-optical mode converter.

$\pm\, 4(\Delta\Omega/2), \pm\, 6(\Delta\Omega/2),\, \cdots$ and in the state B with frequency shifts $\Omega_0 \pm (\Delta\Omega/2)$, $\Omega_0 \pm 3(\Delta\Omega/2)$, $\Omega_0 \pm 5(\Delta\Omega/2)$, $\cdots$ are generated. One can introduce a vector $\mathcal{A} = (A_m)$ with $m = \cdots, -4, -2, 0, 2, 4, \cdots$ for the components at polarization A and another vector $\mathcal{B} = (B_n)$ with $n = \cdots,, -5, -3, -1, 1, 3, 5, \cdots$ for the components at polarization B. According to the coupling scheme only some of the frequency components are directly coupled. Extending the coupled-mode (1) and (2) to the presence of several frequency components, we get the following modified coupling equations

$$\frac{\partial A_m}{\partial z} = -j\kappa^* B_{m+1} \exp\left(-j\delta_1 z\right) - j\kappa^* B_{m-1}$$
$$\cdot \exp\left(-j\delta_2 z\right) \quad \text{with } m \text{ even} \qquad (7)$$

$$\frac{\partial B_n}{\partial z} = -j\kappa A_{n-1} \exp\left(j\delta_1 z\right) - j\kappa A_{n+1}$$
$$\cdot \exp\left(j\delta_2 z\right) \quad \text{with } n \text{ odd} \qquad (8)$$

with $\delta_1 = \beta_{TM} - \beta_{TE} - K_1$ and $\delta_2 = \beta_{TM} - \beta_{TE} - K_2$. The differences of the wavenumbers β_{TM} and β_{TE} for the various frequency components is very small and, therefore, can be neglected in a good approximation. We see from (7) and (8) that in the frequency domain, acousto-optical interaction induced by two acoustic waves creates many components with different frequency shifts for each polarization.

The power of the transmitted optical waves in the polarization state B is given by

$$T_2(t) = \sum_{i,\, k=-\infty}^{\infty} B_i B_k^* \exp\left(j(i-k)\frac{\Delta\Omega}{2} t\right)$$
$$\text{with } i,\, k \text{ odd.} \qquad (9)$$

$T_2(t)$ is a real function in time as for each complex element, e.g., $i = n_1$, $k = n_2$, there exists its complex conjugated element in the sum as well ($i = n_2$, $k = n_1$). Numerical results show that (6) and (9) are exactly equivalent.

To get a better understanding of the mechanism of interchannel interference, we show in the following some numerical results for two-wavelength filtering/switching based on the models developed above. It is clear that the transmission

characteristics depend on the channel separation and the bandwidth of the acousto-optical mode converter. We define the normalized channel separation as

$$NS = \frac{\lambda_2 - \lambda_1}{\text{FWHM}_\lambda} = \frac{\Delta\Omega}{\text{FWHM}_\Omega} \qquad (10)$$

where λ_1 and λ_2 are the center wavelengths of the two channels for which SAW's at Ω_1 and Ω_2, respectively, yield phase-matched conversions. FWHM_λ is the full width at half maximum of the transmission characteristics if operated only with one SAW at a fixed frequency. FWHM_Ω is the full width at half maximum in the acoustical frequency domain which can be obtained if the frequency of the SAW is varied and the transmission of the converted wave at a fixed wavelength is monitored. Similarly, a normalized wavelength (frequency) deviation can be defined as

$$ND = \frac{\delta\lambda}{\text{FWHM}_\lambda} = \frac{\delta\Omega}{\text{FWHM}_\Omega} \qquad (11)$$

with $\delta\lambda$ being the deviation of the wavelength from the wavelength at which phase-matching is exactly fulfilled for the acousto-optical interaction with the SAW at Ω_1 and $\delta\Omega$ being the corresponding frequency deviation of the SAW frequency from Ω_1. In Fig. 3 calculated time evolutions are shown as 3-D diagrams, i.e., the transmission versus the normalized deviation and a normalized time t/T_0. The interaction strengths κ_1 and κ_2 have been assumed to be homogeneous and to give full conversion, i.e., $\kappa_1 = \kappa_2 = \pi/(2\ L)$ (L interaction length), if only one of the SAW's is switched on. The three diagrams have been calculated for a two wavelength operation with $NS = 1$, $NS = 2$ and $NS = 4$, respectively. For larger channel spacings the overall conversion characteristic is (nearly) the sum of two individual characteristics which would appear if only one SAW is present. For narrower channel spacings, however, the individual characterstics are strongly distorted due to the presence of an additional SAW. This results in an amplitude modulation of the power transmission at each individual wavelength channel. Especially for the
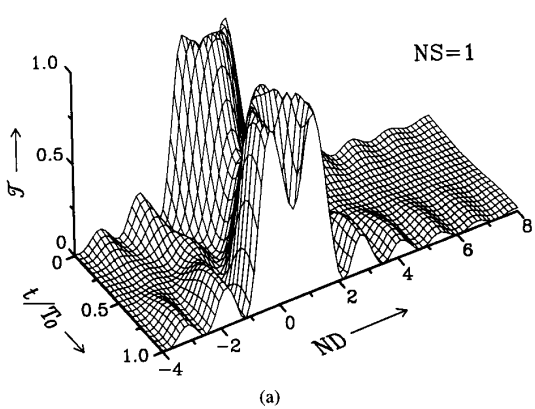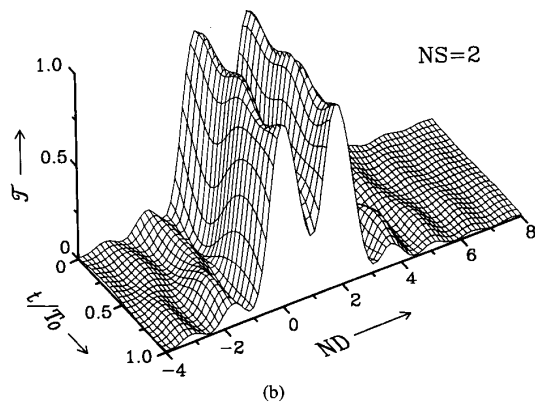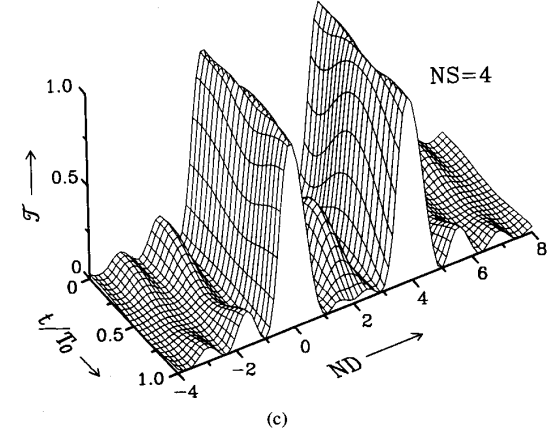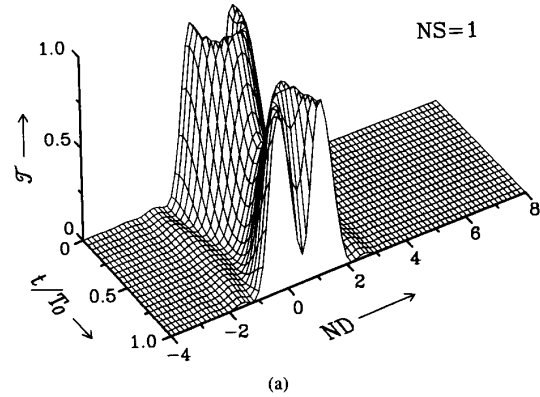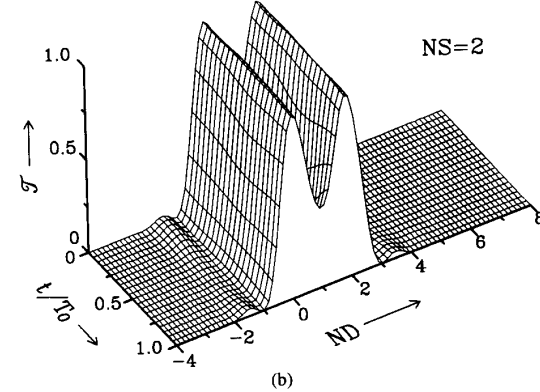
Fig. 3. Calculated time dependence of the conversion characteristics of mode converter with *homogeneous* coupling strength driven by two SAW waves simultaneously. The frequencies of the SAW's are adjusted to yield full conversion at two different wavelengths with (a) $NS = 1$, (b) $NS = 2$, and (c) $NS = 4$, respectively.

Fig. 4. Calculated time dependence of the conversion characteristics of mode converter with *sinusoidally weighted* coupling strength driven by two SAW waves simultaneously. The frequencies of the SAW's are adjusted to yield full conversion at two different wavelengths with (a) $NS = 1$, (b) $NS = 2$, and (c) $NS = 4$, respectively.

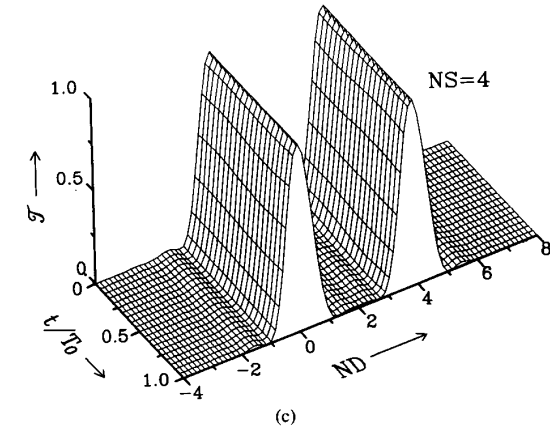narrow spacing corresponding to $NS = 1$ the modulation depth is nearly 50%.

In Fig. 4 similar calculated time evolutions as in Fig. 3 are shown. However, here we have assumed a sinusoidally weighted coupling of the interaction strength. It becomes apparent that for this case the distortions are strongly reduced resulting in a lower modulation depth of the power transmission than in the case of homogeneous coupling.

III. SPECTRAL ANALYSIS OF POWER TRANSMISSION CHARACTERISTICS

To study the effects of interchannel interference we have performed some experiments investigating the characteristics of the power transmission. The results will be discussed in this section and compared with predictions from the theoretical models.

In our experimental setup two RF signals of around 174 MHz have been combined, amplified and applied to an interdigital transducer to excite SAW's at two frequencies (see Fig. 1). The acousto-optical mode converter has been fabricated in X-cut, Y-propagating LiNbO$_3$. The 20-mm-long device consists of a single mode optical waveguide ($\lambda \approx 1.55$ μm) embedded in a low loss ($\approx$0.5 dB/cm) acoustical waveguide resulting in a (nearly) homogeneous coupling strength. A TM-polarized optical wave from a DFB-laser (λ =1556 nm, cw-operation) has been coupled into the converter. The frequency and driving power of the RF$_1$ signal have been adjusted to yield complete polarization conversion for that optical wave without RF$_2$. Afterwards the RF$_2$ signal (with the same power level as RF$_1$) has been switched on and we have measured the power of the converted optical wave (i.e., the TE-polarized wave) behind a polarizer using an InGaAs photodiode. With an RF spectrum analyzer we monitored the frequency components within the signal from the photodiode and observed discrete peaks at the beat frequency and its harmonics. The electrical power of these frequency components has been measured as a function of the frequency separation of the two SAW's.

In Fig. 5(b)–(f) the electrical power of each frequency component is shown as function of the normalized channel separation. Additionally, in Fig. 5(a) the conversion characteristics are drawn as function of the normalized deviation which has been obtained by applying a single SAW and varying its frequency. The solid lines in all diagrams of Fig. 5 show the experimental results, the dashed lines the calculated results obtained from (6) and (9).

The conversion characteristics (a) are sinc^2-like functions. There are some differences between the theoretical and the experimental curves resulting in a slightly lower first sidelobe and a higher second sidelobe of the experimental curve. The origin of these differences is mainly due to inhomogeneities in the structure [15]. In Fig. 5(b) the DC component is shown. The curves start at about -8 dB for narrow separation and increase toward 0 dB for larger spacings. (For $NS = 0$ one gets exactly a complete back conversion into the original polarization state; for the calculated results one has to add up all the frequency components with the correct phases to achieve this result.) The electrical power at frequency $\Delta\Omega$ [Fig. 5(c)] shows some oscillations. However, the function is *not* similar to the conversion characteristics as would be expected from the qualitative description of interchannel interference given in [13]. For narrow channel spacings the amplitudes are at about -14 dB. The functions for the 2$\Delta\Omega$ component start for narrow separations at about -13 dB and monotonically drop down toward larger spacings. The third and fourth order components are only significant if the channel spacing is very narrow (NS <1). There is an excellent agreement between the theoretical and the experimental results.

To overcome or to reduce intensity cross talk cascading of two filters has been successfully demonstrated [5]–[7]. We have investigated such a filter concerning interchannel interference. The filter consists of two acousto-optical mode converters in series separated by an integrated optical TM-pass polarizer. With additional integrated optical TE-pass polarizers
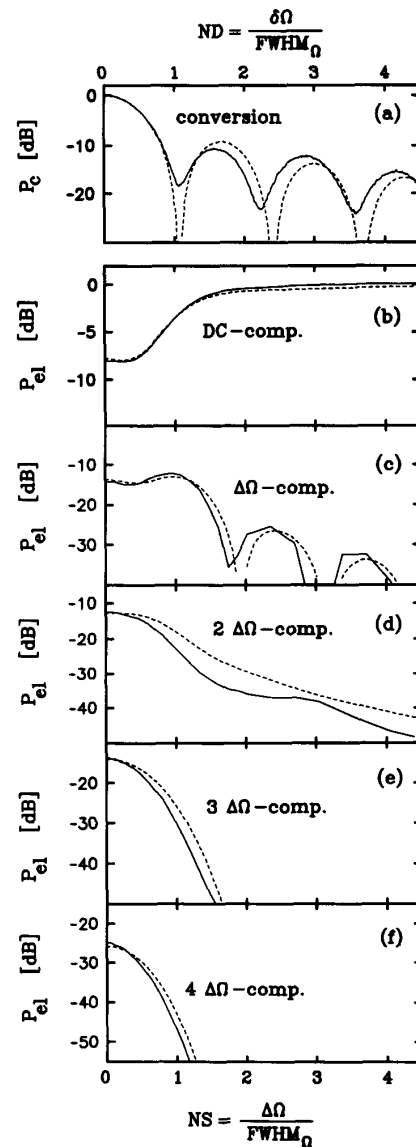

Fig. 5. Electrical power of different frequency components (b)–(f) versus normalized channel separation and the conversion characteristics (a) of a *single stage* acousto-optical mode converter with homogeneous coupling strength versus normalized frequency deviation. The solid and the dashed lines show experimental and calculated results, respectively.

at the input and output of the device, a polarization dependent double stage filter is formed. It allows filter operation for TE-polarized input waves. The interaction lengths of the two acousto-optical mode converters are 10 and 13 mm, respectively. The spectral properties of the device pigtailed with single mode fibers have been investigated using the setup described above.

In Fig. 6(a) the conversion characteristics and in (b)–(f) the electrical power of several frequency components versus the normalized channel separation NS are shown. The solid and the dashed lines show experimental and theoretical results,
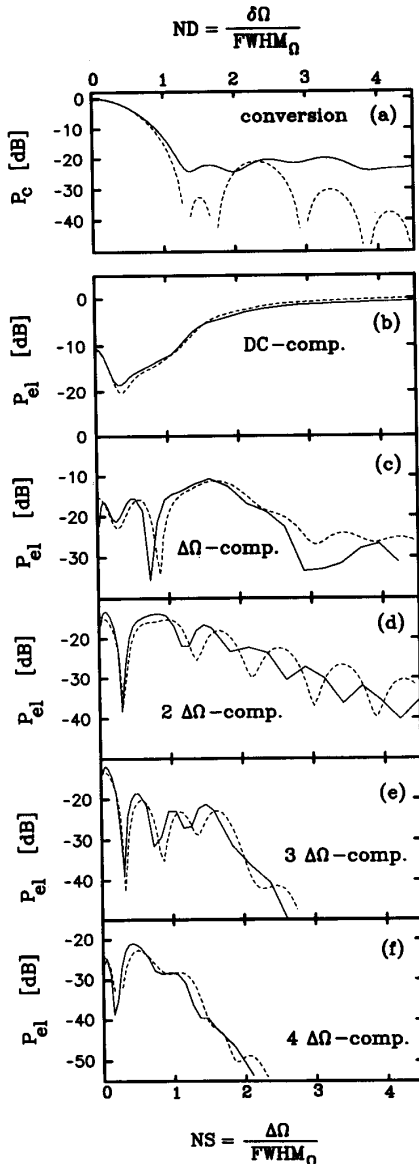
$$ND = \frac{\delta\Omega}{FWHM_0}$$

Fig. 6. Electrical power of different frequency components (b)–(f) versus normalized channel separation and the conversion characteristics (a) of a *double stage* acousto-optical wavelength filter with homogeneous coupling strength versus normalized frequency deviation. The solid and the dashed lines show experimental and calculated results, respectively.

respectively. The experimental conversion characteristic has a baseline floor slightly below −20 dB whereas from the calculated curve a stronger suppression of the sidelobes is expected. The origin of the baseline floor is mainly the nonideal operation of the polarizers allowing a small transmittance even for unconverted waves. The curves for the DC components start at −12 dB for $NS = 0$ and drop down to about −20 dB and afterwards increase monotonically to 0 dB for larger spacings. The other frequency components show always a pronounced dip in the interval between $NS = 0$ and $NS =$

1. The components at $3\Delta\Omega$ and at $4\Delta\Omega$ have significant amplitudes for $NS < 2$ but decrease for larger spacing below −50 dB. The amplitudes of the components at $\Delta\Omega$ and $2\Delta\Omega$, however, are remarkably strong even at large separation. For instance, at a separation of $NS \approx 4$ the amplitudes of the $\Delta\Omega$ component are still in the range of $-20 \cdots -30$ dB. Therefore, some residual amplitude modulation of the transmitted signal occurs even for large channel spacings.

By comparing the experimental results with the calculated curves for the single stage converter as well as for the double stage filter, it is obvious that the predictions from the theoretical models agree well with the experimental results. Of course, there are some residual differences between the curves, but they are mainly due to the nonideal performance of the components, i.e., the polarizer and waveguide homogeneity. Experiments using devices with weighted coupling have not been performed yet, but we expect an improved behavior with a similar good agreement as for the devices with homogeneous coupling.

IV. BER CONSIDERATIONS

The interchannel interference of several acoustic waves in multiwavelength operation of IAOTF's/IAOTS's generates an intrinsic modulation of the transmitted signal of a given wavelength channel. As a consequence, a degradation of the BER occurs resulting in an increase of the required received optical power to maintain the BER. Such a power penalty has already been observed experimentally [13] for a two frequency operation of an acousto-optical mode converter. In this section we analyze the influence on the BER both theoretically and experimentally.

Generally, the bit error rate of a transmission system with on/off-modulation without interchannel interference is given by [16]

$$BER_0(P) = \frac{1}{2}\,\text{erfc}\left(\frac{P}{P_{noise}}\right) \qquad (12)$$

where P is the received optical power and P_{noise} is the noise-equivalent power, which has been assumed to be equal for binary "0" and "1." In the presence of interchannel interference P is modulated. As $\Delta\Omega$ is typically in the range of several hundred kHz, the modulation frequencies are very low in comparison to the frequency components apparent in the transmission signal for moderate or high bit data rates. Therefore, the BER can be calculated by taking the average of $BER_0[P(t)]$ over one modulation period $T_0 = 2\pi/\Delta\Omega$, i.e.:

$$BER = \frac{1}{2T_0}\int_0^{T_0}\text{erfc}\left(\frac{P(t)}{P_{noise}}\right) dt \qquad (13)$$

The time-dependence of $P(t)$ can be calculated using the models described in Section II. In (12) and (13) we have assumed that the decision threshold is at $P/2$. In most practical receiver systems this decision threshold is regulated via a variable preamplifier in a feedback loop depending on the received power level. If its bandwidth is small, the feedback loop can not follow the modulation due to interchannel interference.
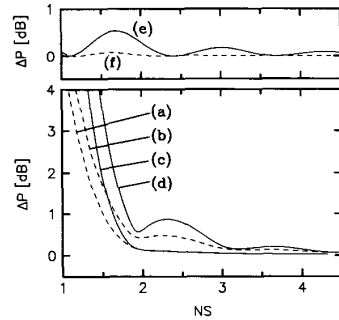
$$NS = \frac{\Delta\Omega}{FWHM_0}$$

Fig. 7. Calculated power penalty ΔP at BER $= 10^{-9}$ of single stage acousto-optical mode converters for two RF-operation versus normalized channel separation (lower diagram). (b) and (d) converter with homogeneous coupling, (a) and (c) converter with sinusoidally weighted coupling. The solid lines have been calculated assuming a low bandwidth feedback loop in the receiver. The upper diagram shows the power penalty due to conventional cross talk, i.e., operation with a single SAW.

In that case the decision threshold P_{th} is determined by the average power level, i.e.

$$P_{th} = \frac{1}{2T_0} \int_0^{T_0} P(t)\, dt \qquad (14)$$

and the BER is given by:

$$\mathrm{BER} = \frac{1}{4}\left[\mathrm{erfc}\left(2\frac{P_{th}}{P_{noise}} \right) \right.$$
$$\left. + \frac{1}{T_0} \int_0^{T_0} \mathrm{erfc}\left(2\frac{P(t) - P_{th}}{P_{noise}} \right) dt \right] \qquad (15)$$

From (13) or (15) the power penalty, i.e., the additional power required to maintain the BER, in comparison with single wavelength operation of an ATOF/ATOS, can be calculated. Whether (13) or (15) must be applied depends on the receiver design of the transmission system.

In the lower part of Fig. 7 the calculated power penalty ΔP at BER $= 10^{-9}$ is shown versus the normalized channel separation for single stage acousto-optical mode converters. The curves (b) and (d) are for mode converters with homogeneous coupling, (a) and (c) for converters with sinusoidally weighted coupling. The dashed lines have been calculated using (13) and the solid lines using (15), i.e., assuming a low bandwidth feedback loop in the receiver. At narrow channel spacings a large power penalty occurs. The penalty for the device with homogeneous coupling is larger than that of the converter with weighted coupling. For receivers with low bandwidth feedback loop the penalty is higher. It is below 1 dB for the homogeneous and weighted coupling for $NS > 1.8$ and $NS > 1.6$, respectively. The functions for the weighted coupling decrease monotonically toward 0 dB for larger separations, whereas the other curves have another slight maximum at about $NS = 2.3$ resulting in a stronger power penalty even at larger separations.

To compare the influence due to interchannel interference with conventional cross talk induced by residual conversion in a neighboring channel, we have calculated the power penalty due to this conventional cross talk. If a single SAW is adjusted to yield complete transmission for one signal, a residual part
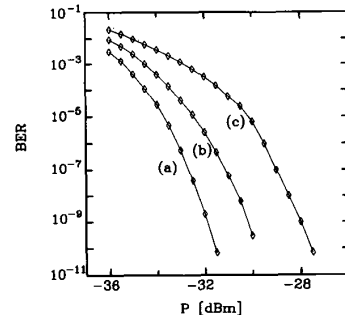

Fig. 8. Measured bit error rate versus received optical power. (a) Operation with single wavelength filtering; (b) and (c) operation with additional RF-signal separated 700 kHz ($NS = 3.9$) and 500 kHz ($NS = 2.8$), respectively.

of the second signal is converted due to the sidelobes of the transmission characteristics resulting in a cross talk. The (worst case) bit error rate is given by

$$\mathrm{BER} = \frac{1}{2}\,\mathrm{erfc}\left(\frac{P_s - P_{cross}}{P_{noise}} \right) \qquad (16)$$

with P_s and P_{cross} being the transmitted power of the desired and cross talk signal, respectively. In the upper part of Fig. 7 the calculated power penalties for homogeneous (e) and weighted coupling (f) are shown. It has been assumed that two optical signals are entering the mode converter with the same power level. It is obvious that the penalties due to conventional cross talk are smaller than that due to interchannel interference.

We have experimentally studied the influence of interchannel interference on BER performance with the double stage filter already discussed in the preceding section. Data transmission experiments with 1.14 Gb/s at $\lambda = 1.56\ \mu$m have been performed. In the transmission system a DFB laser was directly modulated with a $2^{23} - 1$ pseudo random bit sequence and the signal was detected using a pin-diode receiver. We measured the BER as function of the received power level; in Fig. 8 some measured results are shown. The curve (a) shows the BER versus received optical power for the operation with a single SAW, i.e., the frequency and the SAW power had been adjusted to yield maximum transmission at the given wavelength. After exciting a further SAW with the same power level and in frequency 700 kHz (b) and 500 kHz (c) apart (corresponding to $NS = 3.9$ and $NS = 2.8$, respectively), the results shown in curve (b) and (c) have been measured. At BER $= 10^{-9}$ a power penalty of 2.2 dB for the wider spacing and 4.8 dB for 500 kHz separation occurred.

By evaluating several such BER-curves for various frequency separations, it is possible to determine the power penalty as function of the normalized channel separation. The result is shown in Fig. 9. The diamonds mark the experimental results, the dashed and solid lines have been calculated according to (13) and (15), respectively. As our receiver has a low bandwidth feedback loop, the experimental results should be compared with the solid line. In the experiment a slightly larger penalty is observed than theoretically predicted. At about $NS = 3$ the penalty is still 2.2 dB. The differences between the theoretical curve and the experimental results
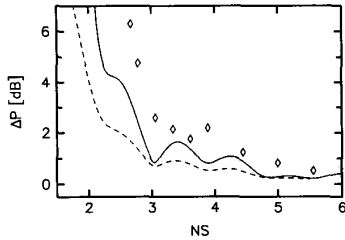
Fig. 9. Power penalty ΔP at BER $= 10^{-9}$ due to two RF-operation of double stage acousto-optical mode converters versus normalized channel separation. The diamonds show experimental results, the dashed and solid lines have been calculated assuming a high and low bandwidth feedback loop in the receiver, respectively.

we attribute mainly to waveguide inhomogeneities resulting in larger sidelobes of the filter curve in each of the stages and, therefore, in a stronger influence of the interchannel interference on the BER degradation even at larger separations.

The results presented in this section, both experimental and theoretical, confirm that interchannel interference strongly influences the system performance. A degradation of the bit error rate characteristics occurs if simultaneous filtering is applied. By comparing the results for single stage and double stage devices it becomes obvious that a stronger degradation occurs for the latter ones. One reason for this is that double stage devices consist of two acousto-optical mode converters. In each of them an amplitude modulation is induced. The overall amplitude modulation is determined by the product of both transmission functions and, therefore, has a larger modulation depth than the single stage transmission function. Similar arguments hold if several filters are cascaded within a transmission line (even at different locations). By comparing weighted and homogeneous coupled devices it becomes clear that with weighted coupling the power penalty is significantly lower for narrow channel separations. Therefore, for system applications in WDM networks devices with weighted coupling strength should be used preferably.

V. CONCLUSION

We have investigated the cross talk induced by interchannel interference in multiwavelength operation of integrated acousto-optical filters and switches. Two models based on coupled mode analysis have been developed to describe multi-wavelength operation in the time and in the frequency domain. An analysis of the frequency spectra of converted waves has been performed both theoretically and experimentally. By comparing both results it could be clearly demonstrated that the theoretical models are well suited to describe multiwavelength operation of IAOTF's/IAOTS's. It has been found that the transmitted signal is amplitude modulated containing several frequency components at multiples of the beat frequency.

Experimental and theoretical investigations of the influence of interchannel interference on system performance in transmission networks have been performed. System degradation resulting in a large power penalty of several dB occurs if the channel spacing is very narrow. The effect is more pronounced in double stage devices than in single stage devices. Especially, in single stage devices with weighted coupling the power

penalty is expected to be neglectable for channel separations larger than about two times the half width of the filter curves.

As the system degradation is a drawback for the applications of IATOF's/IATOS's in WDM networks, further investigations should be performed to reduce the cross talk. For the design of WDM systems with IATOF's/IATOS's the interchannel interference must be taken into account. For dense WDM network nodes special concepts, such as e.g., wavelength dilation [17], must be used.

REFERENCES

[1] K. W. Cheung, "Acousto-optic tunable filters in narrowband WDM networks: System issues and network applications," *IEEE J. Select. Areas Commun.*, vol. SAC-8, pp. 1015–1024, 1990.

[2] H. Herrmann, D. A. Smith, and W. Sohler, "Integrated optical, acoustically tunable wavelength switches and filters and their network applications," in *Proc. 6th Euro. Conf. on Integrated Optics (ECIO'93)*, Neuchatel, Switzerland, Apr. 1993, pp. 10.1–10.3.

[3] G. Hill *et al.*, "A transport network layer based on optical network elements," *J. Lightwave Technol.*, vol. 11, pp. 667–679, 1993.

[4] J. Frangen, H. Herrmann, R. Ricken, H. Seibert, W. Sohler, and E. Strake, "Integrated optical, acoustically tunable wavelength filter," *Electron. Lett.*, vol. 25, pp. 1583–1584, 1989.

[5] D. A. Smith, J. J. Johnson, B. L. Heffner, K.-W. Cheung, and J. E. Baran, "Two stage integrated optic acoustically tunable optical filter with enhanced sidelobe suppression," *Electron. Lett.*, vol. 25, pp. 398–399, 1989.

[6] H. Herrmann, P. Müller-Reich, V. Reimann, R. Ricken, H. Seibert, and W. Sohler, "Integrated optical, TE- and TM-pass, acoustically tunable, double-stage wavelength filter in LiNbO3 ," *Electron. Lett.*, vol. 28, pp. 642–643, 1992.

[7] F. Tian, H. Herrmann, Ch. Leifeld, V. Reimann, R. Ricken, U. Rust, W. Sohler, F. Wehrmann, and S. Westenhöfer, "Polarization independent integrated optical, acoustically tunable double stage wavelength filter in LiNbO3," *J. Lightwave Technology*, vol. 12, pp. 1192–1197, 1994.

[8] K. W. Cheung, S. C. Liew, C. N. Lo, D. A. Smith, J. E. Baran, and J. J. Johnson, "Simultaneous five-wavelength filtering at 2.2 nm separation using acoustooptic tunable filter with subcarrier detection," *Electron. Lett.*, vol. 25, pp. 636–637, 1989.

[9] A. d'Alessandro and D. A. Smith, "Multichannel operation of an integrated acoustooptic wavelength routing switch for WDM systems," *IEEE Photon. Technol. Lett.*, vol. 6, pp. 390–393, 1994.

[10] S. F. Su, R. Olshansky, G. Joyce, D. A. Smith, and J. E. Baran, "Gain equalization in multiwavelength lightwave systems using acoustooptic tunable filters," *IEEE Photon. Technol. Lett.*, vol. 4, pp. 269–271, 1992.

[11] H. Herrmann and St. Schmid, "Integrated acousto-optical mode converters with weighted coupling using surface acoustic wave directional couplers," *Electron. Lett.*, vol. 28, pp. 979–980, 1992.

[12] D. A. Smith and J. J. Johnson, "Sidelobe suppression in an acousto-optic filter with raised-cosine interaction strength," *Appl. Phys. Lett.*, vol. 61, pp. 1025–1027, 1992.

[13] M. M. Choy, K. W. Cheung, D. A. Smith, and J. E. Baran, "Observation of coherent interchannel interference in the multiwavelength operation of an acoustooptic filter," *IEEE Photon. Technol. Lett.*, vol. 1, pp. 171–172, 1989.

[14] H. Nishihara, M. Haruna, and T. Suhara, *Optical Integrated Circuits*. New York: McGraw-Hill, 1989.

[15] D. A. Smith, A. d'Alessandro, J. Baran, and H. Herrmann, "Source of sidelobe asymmetry in integrated acousto-optic filters," *Appl. Phys. Lett.*, vol. 62, pp. 814–816, 1993.

[16] I. Andonovich and D. Uttamchandani, *Principles of Modern Optical Systems*. Norwood, MA: Artech House, 1989.

[17] J. Sharony, K.-W. Cheung, T. E. Stern, "The wavelength dilation concept in lightwave networks—Implementation and system considerations," *J. Lightwave Technol.*, vol. 11, pp. 900–907, 1993.
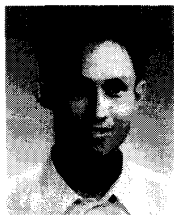
Feng Tian received the B.S. degree in optoelectronics from the University of Electronic Science and Technology, Chengdu/China, in 1982, and the M.S. and Ph.D. degrees in electrical engineering from Beijing University of Posts and Telecommunication, Beijing/China in 1984 and 1988, respectively.

From 1984–1990 he was with the Optical Communications Laboratory of Beijing University of Posts and Telecommunications. In 1990 he joined the Department of Applied Physics of the University of Paderborn/Germany as an Alexander-von-Humboldt research fellow pursuing the research on integrated optical sensing technology. Since 1992 he has been working in Paderborn within the European RACE-project "Multi-Wavelength Transport Network." His research interests include optical communication and component technology.

Harald Herrmann was born in Martfeld/Germany in 1958. He received the diploma degree in physics from the University of Hannover in 1984.

The same year he joined the Department of Applied Physics of the University of Paderborn/Germany. There he was engaged in the development of color center lasers and in investigations of nonlinear processes in integrated optical waveguides and new electro-optical and acousto-optical devices. In 1991 he received the Ph.D. degree (Dr. rer. nat.) with a thesis on nonlinear difference frequency generation in lithium niobate waveguides. He currently works on integrated acousto-optical devices and their applications in optical communication systems and optical instrumentation.

Dr. Herrmann is a member of the German Physical Society.